*Scientific Journal of Impact Factor (SJIF): 5.71*

e-ISSN (O): 2348-4470
p-ISSN (P): 2348-6406

**International Journal of Advance Engineering and Research Development**

*International Conference on Momentous Role of Nanomaterials in Renewable Energy Devices*

*Volume 5, Special Issue 07, April-2018 (UGC Approved)*

# Synthesis and Characterization of γ-$Bi_2O_3$ Nanorods

B. Jansi Rani[1], G. Ravi[1], R. Yuvakkumar[1]*

[1]*Nanomaterials Laboratory, Department of Physics, Alagappa University, Karaikudi, Tamil Nadu 630 003, India*
*E-mail:- yuvakkumar@gmail.com*

***Abstract*** *- γ-$Bi_2O_3$ nanorods have been successfully synthesized by facile one pot hydrothermal route. The formation of body centered cubic structure of γ-$Bi_2O_3$ has been confirmed through X-ray diffractometer (XRD) results. Four defined Raman active modes have been reported from Raman spectral analysis. The photoluminescence (PL) spectra revealed the presence of oxygen vacancies in the synthesized sample from the peaks centered at 422, 453 and 481. The metal oxygen vibration (Bi-O) modes of γ-$Bi_2O_3$ nanorods exposed from Fourier transform infrared (FTIR) spectroscopy result by the bands centered at 514 $cm^{-1}$. The nanorods surface morphology of synthesized γ-$Bi_2O_3$ has been evaluated by scanning electron micrograph (SEM) images. The successful phase controlled synthesis and characterization of γ-$Bi_2O_3$ nanorods have been reported in this work.*

***Keywords-*** *γ-$Bi_2O_3$ nanorods; Morphology evolution; Phase controlled synthesis.*

## I. INTRODUCTION

In general, bismuth oxide nanostructures with different morphology and various dimensions like 1D nanorods, nanotubes, nanowires, 2D nanoplates, nanoflakes and 3D hierarchical nanoflowers etc have owned many peculiar and unique physical and physico-chmeical properties [1]. Especially, due to its band gap, high oxygen conductive nature and noticeable luminescent behavior and appreciable photo conducting properties were made it to adapt many recent research areas like gas sensors, dielectric materials, photocatalyst and water splitting application etc [2]. There are three different polymorphs can be synthesized in $Bi_2O_3$ nanostructures such as α-, β- and γ-$Bi_2O_3$ holding the crystal structures monoclinic, tetragonal and cubic respectively. Each differs by its phase, structure, morphology and properties. Among them, cubic γ-$Bi_2O_3$ nanostructures possessed the surface defects and excellent photocatalytic activity which attracts the attention of modern researchers [3]. Still it is challenged to the researchers to stabilize the γ phase of $Bi_2O_3$. Many research groups are working towards the controllable synthesis of γ-$Bi_2O_3$ nanostructures for various efficient performances in energy related fields. Recently, Kuan Li and team proposed the facile route to prepare and stabilize the γ-$Bi_2O_3$ phase photocatalyst by adding surfactant and commended its photocatalytic performance [4]. Yajun Wang and research group worked on controllable synthesis of metastable γ-$Bi_2O_3$ architectures and optical properties successfully [5]. Ling Li and coworkers synthesized $In^{3+}$-stabilized γ-$Bi_2O_3$ sillenite semiconductor with cation deficiency and investigated its optical performance [6]. Sonkusare et al explored the microwave-mediated synthesis of α-$Bi_2O_3$ microflowers/novel γ-$Bi_2O_3$ microspindles and revealed its photocatalytic degradation and antibacterial activity successfully [7]. Ahila and research team investigated the optical properties of *Codium tomentosum* seaweed like $Bi_2O_3$ nanostructure and reported its gas-sensing activity [8]. Malligavathy and co-workers analyzed the phase purity and optical studies of $Bi_2O_3$ nanoparticles suitable for photocatalytic activity [9]. Guo Liu and group worked on controllable synthesis of α-$Bi_2O_3$ and γ-$Bi_2O_3$ with high photocatalytic activity by α-$Bi_2O_3$/ γ-$Bi_2O_3$/ α-$Bi_2O_3$ transformation in a facile precipitation method [10]. Stimulated by these works, we focused to explore the controlled synthesis of cubic γ-$Bi_2O_3$ phase by low temperature calcinations and also we successfully controlled the 1D nanorod morphology of cubic γ-$Bi_2O_3$ by simple one pot hydrothermal route in this work. Further, the confirmation of phase, morphology and optical properties of the synthesized γ-$Bi_2O_3$ nanorods have been established by carried out XRD, SEM, Raman, PL and FTIR studies respectively.

## II. MATERIALS AND METHODS

Analytical grade $Bi(NO_3)_3.5H_2O$, $HNO_3$, NaOH, $C_2H_5OH$, deionized water and Whatmann filter sheet were purchased from Sigma Aldrich and used without further purification. Initially, 1M of $Bi(NO_3)_3.5H_2O$ was dissolved in 35 ml of $HNO_3$ (1 mol/L) under magnetic stirring of rpm 600 for 30 minutes. Then 2M of NaOH dissolve in 35 ml of deionized water was added drop wise in to the above solution forms milk color fine colloid. This mixed colloidal solution was continued in stirrer condition for 1 h. Finally, the solution was transformed in to 100 ml Teflon lined autoclave which was

maintained in 100°C for 24 h. After naturally cooled to room temperature, the powder was then cleaned with absolute ethanol and water for five times to get rid of the precursor residues. Then the powder was dried in hot air oven at 80°C overnight. The dried powder was calcinated at 500°C for 3 h to obtain γ-$Bi_2O_3$ nanorods. The finally obtained γ-$Bi_2O_3$ nanorods have been characterized by the following studies. X-ray powder diffraction (X'pert PRO analytical diffractometer) using CuKα as radiation (1.541 A˚) source was carried out to confirm the phase and crystalline nature of the sample. Imaging Spectrograph STR 500 nm focal length laser micro Raman spectrometer SEKI, Japan with resolution: 1/0.6 cm-1/pixel and Flat Field: 27 mm (W) × 14 mm (H) was carried to confirm the phonon active modes present in the sample. The luminescent behavior of the sample has been analyzed by photoluminescence (PL) spectrum measured using Varian Cary Eclipse Photoluminescence Spectrometer with Oxford low temperature LN2 77K setup. The metal oxygen and other functional group vibrations present in the sample were confirmed by Infrared (IR) spectra recorded using Fourier transform infrared spectrophotometer using Thermo Nicolet 380 with resolution 0.5 cm-1 and S/N ratio: 2000:1 ppm for 1 minute scan. The nanorod morphology was examined by carried out Scanning Electron Microscope (ZEISS-V80).

## III. RESULTS AND DISCUSSION

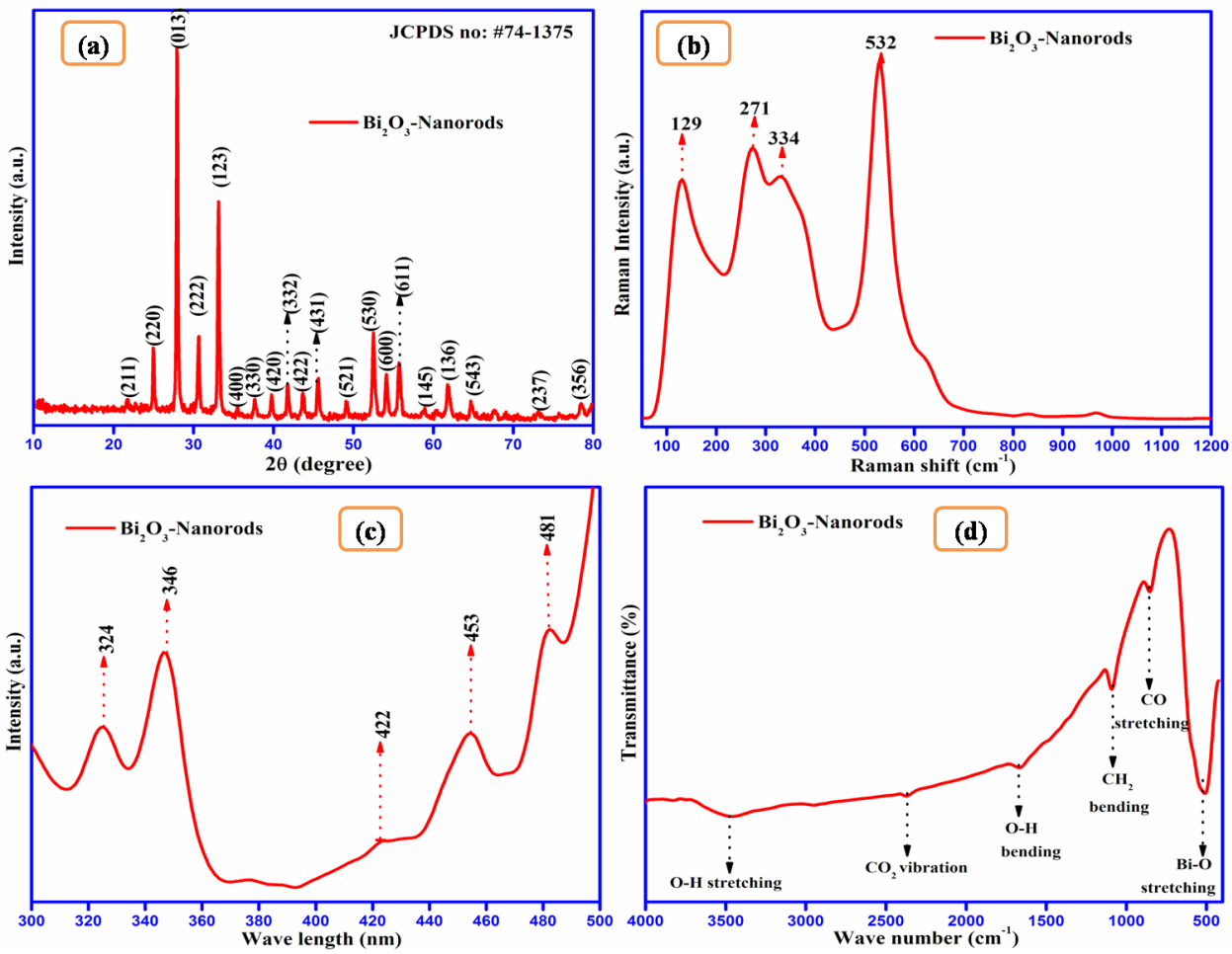


***Figure 1.*** *(a) XRD (b) Raman(c) PL (d) FTIR pattern of γ-$Bi_2O_3$ Nanorods*

***Table 1.*** *Cryastallite size and lattice constant determination*

| Sample | Pos. [°2Th.] | FWHM Left [°2Th.] | d-spacing [A] | Lattice constant (nm) | Crystallite size (nm) |
|---|---|---|---|---|---|
| γ-$Bi_2O_3$ | 27.92 | 0.1968 | 3.23856 | 1.024 | 41.62 |

Figure 1 (a) represents the XRD pattern of cubic γ-$Bi_2O_3$ nanorods which revealed the high crystalline nature of sample. The body centered cubic structure of γ-$Bi_2O_3$ has been confirmed through the displayed diffraction peaks in XRD. The peaks centered at 2θ values at 21.59, 24.98, 27.92, 30.75, 33.25, 35.61, 37.86, 39.99, 42.12, 43.97, 45.89, 49.51, 52.98, 54.56, 56.41, 59.35, 62.47, 65.44, 73.96 and 79.47$^o$ correspond to the crystal planes (211), (220), (013), (222), (123), (400), (330), (420), (332), (422), (431), (521), (530), (600), (611), (145), (136), (543), (237) and (356) respectively which were perfectly coincided with the JCPDS data card no: #74-1375 of body centered cubic γ-$Bi_2O_3$ nanostructures. No other peaks none other than characteristic peaks present in XRD. The well defined sharp diffraction peaks denoted the pure phase high crystallinity of the sample. The average crystallite size of the sample can be determined from Debye-Scherer formula: **$D = 0.9\lambda/\beta \cos\theta$;** where λ is the X-ray wavelength, β is the full width at half maximum intensity and θ is the Bragg's angle. The crystallite size of the obtained product is 41.62 nm and the lattice constant of the sample was calculated as 1.024 nm by using the formula: **$a = d\,(h^2+k^2+l^2)^{1/2}$** where h, k and l are miller indices of the crystal planes as shown in Table.1. Raman spectrum of the synthesized cubic γ-$Bi_2O_3$ nanorods has been displayed in figure 1(b). Well predictable four Raman active vibration modes observed at 129, 271, 334 and 532 $cm^{-1}$ could be attributed to the characteristic phonon vibration modes of intrinsic cubic γ-$Bi_2O_3$ nanostructures reported in literature [11]. Since Raman analysis again strongly evidenced the formation of γ-$Bi_2O_3$ nanostructure. The luminescent behavior of the sample revealed by photoluminescence (PL) spectrum in figure 1(c) which shows five emission peaks at 324, 346, 422, 453 and 481 nm correspond to the excitation wavelength of 280 nm given to the sample. The peak at 324 and 346 falls in UV region may due to band edge emission. The blue emission at 453 nm with minor shoulder peak at 422 nm and the blue green emission at 481 nm of γ-$Bi_2O_3$ nanorods are similar as that of the PL spectra of body centered γ-$Bi_2O_3$ nanostructures reported in literature [12]. The presence of shoulder peak attributed to the band to band recombination of direct transition of cations. The luminescent nature of γ-$Bi_2O_3$ is mainly due to the intraionic transition of $Bi^{3+}$ and $Bi^{2+}$ cations. Further the blue green emission merely contributed due to the oxygen vacancies present in the sample which assigned to $^2P_{3/2}(1)\rightarrow{}^2P_{1/2}$ transition or it may due to the transition of charge transfer between the ligands and $Bi^{3+}$ ions [13]. The overall inhomogeneous of PL spectrum observed for the sample may due to the surface defects attributed to the sample. The metal oxygen vibration and the presence of other functional groups present in the sample revealed by Fourier transform infrared (FTIR) spectrum in figure 1(d). The metal oxygen vibration at 514 $cm^{-1}$ corresponds to Bi-O stretching vibration [14]. The other vibrations at 906, 1076, 1650, 2360 and 3453 $cm^{-1}$ correspond to CO stretching, $CH_2$ bending, OH bending, atmospheric $CO_2$ vibration and OH stretching vibrations respectively [15-19]. Hence FTIR spectrum of synthesized synthesized sample confirmed the formation of gamma phase cubic γ-$Bi_2O_3$.

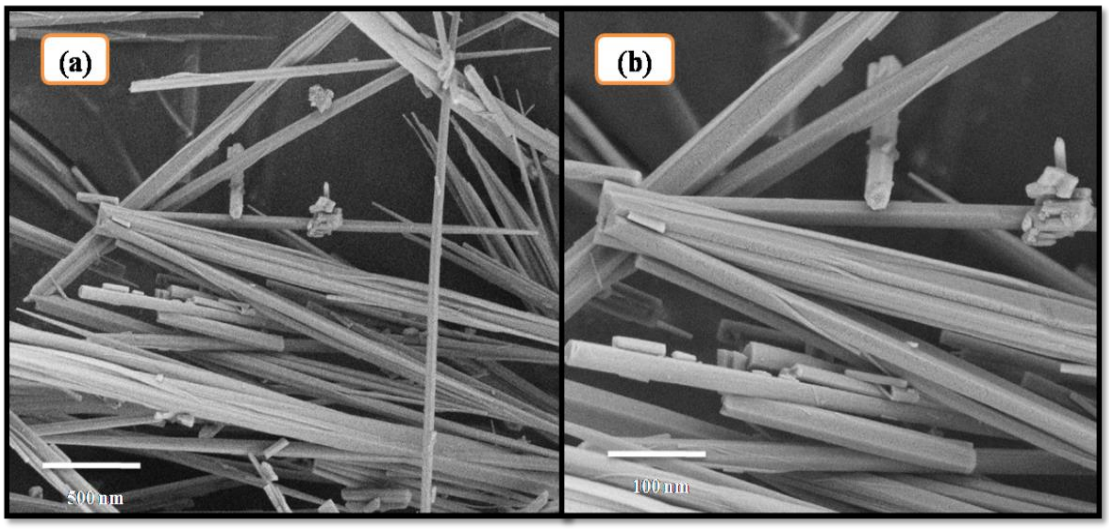


***Figure 2.*** *SEM images of γ-$Bi_2O_3$ Nanorods (a) at 500 nm (b) at 100 nm scale range*

The surface morphology of the synthesized γ-$Bi_2O_3$ has been evaluated by scanning electron micrograph (SEM) images in different nanometer scale range such as 500 and 100 nm respectively shown in figure 2. Highly oriented more functionalized finite 1D nanorod morphology is achieved by maintaining the optimum temperature and pressure condition of hydroythermal route. Specifically oriented self assembly of nanorods is illustrated in SEM images of the sample. This kind of defined 1D morphology supports the easiest charge transportation for much kind of energy related applications such as super capacitors, OER activity, photocatalytic and water splitting applications etc.

## IV. CONCLUSION

Facile one step hydrothermal route was adapted to synthesize the body centered cubic γ-$Bi_2O_3$ nanorods successfully in this work. The controlled synthesis parameters and optimum temperature, pressure condition and calcinations was maintained to achieve well defined 1D nanostructure of metastable cubic γ-$Bi_2O_3$ phase. Hence this one step facile protocol is suggested to synthesis the excellent oxygen vacancies rich cubic γ-$Bi_2O_3$ 1D nanorods for many potential applications.

## ACKNOWLEDGEMENT

This work was supported by UGC Start-Up Research Grant No.F.30-326/2016 (BSR).

## REFERENCES

[1] H. X. Li, Z. F. Bian, J. Zhu, D. Q. Zhang, G. S. Li, Y. N. Huo, H. Li and Y. F. Lu, "Mesoporous titania spheres with tunable chamber structure and enhanced photocatalytic activity," *J. Am. Chem. Soc*. 129, 8406-8407, 2007.
[2] L. Liu, W. Liu, X. L. Zhao, D. M. Chen, R. S. Cai, W. Y. Yang, S. Komarneni, D. J. Yang, "Selective capture of iodide from solutions by microrosette-like δ-$Bi_2O_3$," *ACS Appl. Mater. Inter*. 6, 16082-16090, 2014.
[3] C. Yu, W. Zhou, L. Zhu, G. Li, K. Yang and R. Jin, "Integrating plasmonic Au nanorods with dendritic like α-$Bi_2O_3$/$Bi_2O_2CO_3$ heterostructures for superior visible-light-driven photocatalysis" *Appl. Catal. B*, 184**,** 1-11, 2016.
[4] K. Li, S. Li, J. Zhang, Z. Feng and C. Li, "Preparation and stabilization of γ-$Bi_2O_3$ photocatalyst by adding surfactant and its photocatalytic performance," *Mater. Res. Express*, 4**,** 065902, 2017.
[5] Y. Wang, Z. Li, H. Yu and L. Guo, "Controllable synthesis of metastable γ-$Bi_2O_3$ architectures and optical properties, *Materials Science in Semiconductor Processing*, 64 (2017) 55-62
[6] L. Li, L. Meng, F. Wang and Y. Wang, "Synthesis and optical characterization of $In^{3+}$-stabilized γ-$Bi_2O_3$ sillenite semiconductor with cation deficiency," *Mater. Sci. Semicond. Process*, 68, 48-52, 2017.
[7] V. N. Sonkusare, R. G. Chaudhary, G. S. Bhusari, A. R. Rai and H. D. Juneja, "Microwave-mediated synthesis, photocatalytic degradation and antibacterial activity of α-$Bi_2O_3$ microflowers/novel γ -$Bi_2O_3$ microspindles," *Nano-Structures & Nano-Objects*, 13, 121-131, 2018.
[8] M. Ahila, E. Subramanian and D. Pathinettam Padiyan, "Optical properties of Codium tomentosum seaweed like $Bi_2O_3$ nanostructure and its gas-sensing activity," *Ionics*, DOI: 10.1007/s11581-017-2331-3.
[9] M. Malligavathy and D. Pathinettam Padiyan, "Phase Purity Analysis and Optical Studies of $Bi_2O_3$ Nanoparticles Suitable for Photocatalytic Activity," *Int. J. Nanoscience*, 16, 1760040, 2017.
[10] G. Liu, S. Li, Y. Lu, J. Zhang, Z. Feng, C. Li, "Controllable synthesis of α-$Bi_2O_3$ and γ-$Bi_2O_3$ with high photocatalytic activity by α-$Bi_2O_3$/γ-$Bi_2O_3$/α-$Bi_2O_3$ transformation in a facile precipitation method," *J. Alloys Compds*. 689, 787-799, 2016.
[11] S. J. A. Moniz, C. S. Blackman, C. J. Carmalt and G. Hyett, "MOCVD of crystalline $Bi_2O_3$ thin films using a single-source bismuth alkoxide precursor and their use in photodegradation of water," *J. Mater. Chem*. 20, 7881-7886, 2010.
[12] Y. Wanga and Y. Li, "Metastable γ-$Bi_2O_3$ tetrahedra: Phase-transition dominated by polyethylene glycol, photoluminescence and implications for internal structure by etch," *J. Colloid Interface Sci*. 454, 238-244, 2015.
[13] Y. Zorenko, V. Gorbenko, T. Voznyak, V. Jary and M. Nikl, "Luminescence spectroscopy of the $Bi^{3+}$ single and dimer centers in $Y_3Al_5O_{12}$: Bi single crystalline films," *J. Lumin*. 130, 1963-1969, 2010.
[14] Y. Sun, W. Wang, L. Zhang and Z. Zhang, "Design and controllable synthesis of α-/γ-$Bi_2O_3$ homojunction with synergetic effect on photocatalytic activity," *Chem. Eng. J*. 211-212, 161-167, 2012.
[15] B. J. Rani, S. P. Raj, B. Saravanakumar, G. Ravi, V. Ganesh, S. Ravichandran and R. Yuvakkumar, "Controlled synthesis and electrochemical properties of Ag-doped $Co_3O_4$ nanorods," *Int J Hydrogen Energy*, 42, 29666-29671, 2017.
[16] K. J. Ramalingam, N. R. Dhineshbabu, S. R. Srither, B. Saravanakumar Electrical measurement of PVA/graphene nanofibers for transparent electrode applications, *Synthetic Metals*, 191, 113-119, 2014.
[17] G. Karunakaran, R. Suriyaprabha, P. Manivasakan, R. Yuvakkumar, Impact of nano and bulk ZrO2, TiO2 particles on soil nutrient contents and PGPR, *Journal of nanoscience and nanotechnology*, 13 (1), 678-685, 2013.
[18] R. Yuvakkumar, S. I, Hong, Nd2O3: novel synthesis and characterization, *Journal of Sol-Gel Science and Technology*, 73 (2), 511-517, 2015.
[19] D. S. Priya, R. Suriyaprabha, R. Yuvakkumar, V. Rajendran, Chitosan-incorporated different nanocomposite HPMC films for food preservation, *Journal of nanoparticle research*, 16 (2), 2248, 2014.